

An effective QCD Lagrangian in the presence of an axial chemical potential

A. A. Andrianov^{1,2}, D. Espriu² and X. Planells²

¹ V. A. Fock Department of Theoretical Physics, Saint-Petersburg State University,
 198504 St. Petersburg, Russia

² Departament d'Estructura i Constituents de la Matèria and
 Institut de Ciències del Cosmos (ICCUB), Universitat de Barcelona,
 Martí i Franquès 1, 08028 Barcelona, Spain

October 2012

Abstract

We consider the low energy realization of QCD in terms of mesons when an axial chemical potential is present; a situation that may be relevant in heavy ion collisions. We shall demonstrate that the presence of an axial charge has profound consequences on meson physics. The most notorious effect is the appearance of an explicit source of parity breaking. The eigenstates of strong interactions do not have a definite parity and interactions that would otherwise be forbidden compete with the familiar ones. In this work we focus on scalars and pseudoscalars that are described by a generalized linear sigma model. We comment briefly on the screening role of axial vectors in formation of effective axial charge and on the possible experimental relevance of our results, whose consequences may have been already seen at RHIC.

1 Introduction

The possibility that in extreme conditions QCD breaks parity has been in the past years actively investigated. Indeed invariance under parity is one of the characteristic footprints of strong interactions. Yet there are reasons to believe that this symmetry may be broken in Nature at least in two different settings.

The first possibility is likely to occur in environments with a large baryonic chemical potential. In this case the fermionic determinant in the QCD partition function is not anymore positive definite and the studies that indicate that parity cannot be spontaneously broken [1] for $\mu_B = 0$ simply do not apply at $\mu_B \neq 0$. In fact analytical studies with effective meson lagrangians realizing all the QCD properties at low energies suggest that there is a definite window of baryonic chemical potentials leading to a vacuum where parity is spontaneously broken [2]. Unfortunately it is difficult to verify these results numerically using lattice field techniques due to the notorious problems that finite density numerical simulations present [3].

A second possibility has been abundantly discussed in recent times in connection with the so-called Chiral Magnetic Effect [4]. It is believed that thermal fluctuations may induce topological charge fluctuations in the gauge configuration [5, 6] ΔT_5 and they are detected on lattices [7]. This leads to an effective ' θ -term' in the effective action that in turn induces a coupling between the electric and the magnetic fields, leading to the production of positively and negatively charged particles in opposite directions. It has been claimed that this signal is observed in the STAR experiment at RHIC

[8], although the issue still remains controversial. In addition the precise mechanism of creation of a sufficiently intense topological fluctuation is also unclear at present.

This fluctuation, if extended over the whole fireball, may live for a sufficiently long time to generate in practice a metastable state characterized by a topological chemical potential μ_θ . If this is the case, in a finite volume and only for light quarks, the topological chemical potential can be transformed into a chiral chemical potential μ_5 thanks to the anomalous PCAC equation

$$\partial^\mu J_{5,\mu} - 2i\bar{q}\hat{m}_q\gamma_5 q = \frac{N_f}{2\pi^2}\partial^\mu K_\mu, \quad (1)$$

where

$$K_\mu = \frac{1}{2}\epsilon_{\mu\nu\rho\sigma}\text{Tr}\left(G^\nu\partial^\rho G^\sigma - i\frac{2}{3}G^\nu G^\rho G^\sigma\right), \quad (2)$$

and

$$\Delta T_5 = T_5(t_f) - T_5(0) = \frac{1}{4\pi^2}\int_0^{t_f} dt \int_{\text{vol.}} d^3x \partial^\mu K_\mu. \quad (3)$$

If $m_q \simeq 0$ and no zero modes are present due to the finiteness of the volume then one gets,

$$\frac{d}{dt}(Q_5^q - 2N_f T_5) \simeq 0, \quad Q_5^q = \int_{\text{vol.}} d^3x \bar{q}\gamma_0\gamma_5 q. \quad (4)$$

This is the physical situation we will consider in the present work. In any case, it seems interesting to investigate how hadronic physics is modified by the presence of μ_5 .

This paper is organized as follows. In Sec. 2 a generalized Σ model is presented. Mass-gap equations for three v.e.v. of neutral scalar fields are derived and solved analytically. Then we determine the best fit of parameters of the model comparing with the experimental inputs for scalar and pseudoscalar meson spectral data [9]. In Sec. 3 the axial chemical potential is introduced and treated as a constant time component of an isosinglet axial-vector field in the non-strange sector. We obtain the modification of the mass-gap equations and find the distortion of a_0 - and π - meson spectra caused by the parity breaking. In Sec. 4 a more complicated mixing of three meson states, σ , η , η' , is investigated when the medium has an axial charge. At certain energies some particle states become tachyons (recall we are in-medium so this actually does not represent a fundamental problem). In Sec. 5 all decay widths are calculated for both the rest frame and for moving particles (we note that when axial charge fills the medium, the Lorentz invariance is broken). In Sec. 6 the problem of isosinglet axial-vector meson condensation and its interference with the axial chemical potential is examined. Sec. 7 is devoted to our conclusions and outlook.

2 Generalized Σ model

Our starting point will be the following Lagrangian, invariant under $SU(3)_F$

$$\begin{aligned} \mathcal{L} = & \frac{1}{4}\text{Tr}(D_\mu H D^\mu H^\dagger) + \frac{b}{2}\text{Tr}[M(H + H^\dagger)] + \frac{M^2}{2}\text{Tr}(HH^\dagger) - \frac{\lambda_1}{2}\text{Tr}[(HH^\dagger)^2] - \frac{\lambda_2}{4}[\text{Tr}(HH^\dagger)]^2 \\ & + \frac{c}{2}(\det H + \det H^\dagger) + \frac{d_1}{2}\text{Tr}[M(HH^\dagger H + H^\dagger H H^\dagger)] + \frac{d_2}{2}\text{Tr}[M(H + H^\dagger)]\text{Tr}(HH^\dagger) \end{aligned} \quad (5)$$

where $H = \xi\Sigma\xi$, $\xi = \exp\left(i\frac{\Phi}{2f}\right)$, $\Phi = \lambda^a\phi^a$ and $\Sigma = \lambda^b\sigma^b$. This model can be confronted to similar models in [10, 11, 12] with the important difference (see below) in the trilinear vertices with couplings d_1, d_2 . The neutral v.e.v. of the scalars are defined as $v_i = \langle\Sigma_{ii}\rangle$ where $i = u, d, s$, and satisfy the following gap equations:

$$M^2 v_i - 2\lambda_1 v_i^3 - \lambda_2 v_i^2 v_j + c \frac{v_u v_d v_s}{v_i} = 0. \quad (6)$$

For further purposes we need the non-strange meson sector and η_s . In terms of v.e.v. and physical scalar and pseudoscalar states, the parametrization used here is

$$\Phi = \begin{pmatrix} \eta_q + \pi^0 & \sqrt{2}\pi^+ & 0 \\ \sqrt{2}\pi^- & \eta_q - \pi^0 & 0 \\ 0 & 0 & \sqrt{2}\eta_s \end{pmatrix}, \quad \Sigma = \begin{pmatrix} v_u + \sigma + a_0^0 & \sqrt{2}a_0^+ & 0 \\ \sqrt{2}a_0^- & v_d + \sigma - a_0^0 & 0 \\ 0 & 0 & v_s \end{pmatrix}. \quad (7)$$

The mixing among η 's is defined via the ψ angle

$$\begin{pmatrix} \eta_q \\ \eta_s \end{pmatrix} = \begin{pmatrix} \cos \psi & \sin \psi \\ -\sin \psi & \cos \psi \end{pmatrix} \begin{pmatrix} \eta \\ \eta' \end{pmatrix}. \quad (8)$$

As stated in the introduction, an axial charge can only be effectively generated for nearly massless quarks. Therefore we exclude kaons and their scalar partners κ from the analysis. Let us take for the time being $\mu_5 = 0$ and assume $v_u = v_d = v_s = v_0 \equiv f_\pi \approx 92$ MeV because we only consider the effect of masses perturbatively. As a function of the Lagrangian parameters, the main physical magnitudes derived from this model are

$$\begin{aligned} v_0 &= \frac{c \pm \sqrt{c^2 + 4M^2(2\lambda_1 + 3\lambda_2)}}{2(2\lambda_1 + 3\lambda_2)}, & m_\pi^2 &= \frac{2}{v_0}(b + (d_1 + 3d_2)v_0^2)m, \\ m_a^2 &= 2(-M^2 + 3(2\lambda_1 + \lambda_2)v_0^2 + cv_0 - 2(3d_1 + 2d_2)mv_0 - 2d_2m_s v_0), \\ m_\sigma^2 &= 2(-M^2 + (6\lambda_1 + 7\lambda_2)v_0^2 - cv_0 - 6(d_1 + 2d_2)mv_0 - 2d_2m_s v_0), \\ m_{\eta,\eta'}^2 &= \frac{m_\pi^2}{2m}(m + m_s) + 3cv_0 \mp \sqrt{8c^2v_0^2 + \left[\frac{m_\pi^2}{2m}(m - m_s) + cv_0\right]^2}, \\ \Gamma_a^2 &= \frac{(-4m_\eta^2 m_\pi^2 + (-m_a^2 + m_\eta^2 + m_\pi^2)^2)(m_a^2 - m_\eta^2 + 4d_1 m v_0)^4}{(48m_a^3 \pi v_0^2)^2}, \\ \Gamma_\sigma^2 &= \frac{9(m_\sigma^2 - 4m_\pi^2)(m_\sigma^2 - m_\pi^2 + 4(d_1 + 2d_2)mv_0)^4}{(32m_\sigma^2 \pi v_0^2)^2}, \\ \sin(2\psi) &= \frac{4\sqrt{2}cv_0}{m_{\eta'}^2 - m_\eta^2}, \end{aligned} \quad (9)$$

with $m/m_s = (m_u + m_d)/(2m_s) \simeq 1/25$. The angle ψ is not really necessary for our subsequent discussion but it will be eventually useful in the computation of Dalitz decays and we can use it as a test of the model. v_0 is found via gap equations. These equations are inserted in MINUIT in order to find the minimum of the χ^2 estimator using the following experimental numbers (in MeV):

$$\begin{aligned} v_0^{\text{exp}} &= 92 \pm 5, & m_\pi^{\text{exp}} &= 137 \pm 5, & m_a^{\text{exp}} &= 980 \pm 50, \\ m_\sigma^{\text{exp}} &= 600 \pm 120, & m_\eta^{\text{exp}} &= 548 \pm 50, & m_{\eta'}^{\text{exp}} &= 958 \pm 100, \\ \Gamma_a^{\text{exp}} &= 60 \pm 30, & \Gamma_\sigma^{\text{exp}} &= 600 \pm 120. \end{aligned} \quad (10)$$

The σ mass is assumed to be relatively large as we are not considering any glueballs, so this σ is a sort of average of the real σ and other 0^+ light states. We have assigned generous error bars to include the uncertainties in the model itself. In the minimization process there are several control variables:

- The value of the potential in the minimum has to be $V(v_0) < 0$ since $v = 0$ is an extremal point with $V(v = 0) = 0$ but in the case the latter is a minimum, the true vacuum has to have a lower energy. Also, there is a control of the third extremal, which has to be higher than the true minimum.

$$V(v_0) = \frac{1}{4}v_0^2(-6M^2 + 3(2\lambda_1 + 3\lambda_2)v_0^2 - 4cv_0)$$

- The Hessian matrix has degenerate eigenvalues and there are only two different eigenvalues whose positivity should be provided

$$(V'')_1(v_0) = -M^2 + 3(2\lambda_1 + \lambda_2)v_0^2 + cv_0,$$

$$(V'')_2(v_0) = -M^2 + 3(2\lambda_1 + 3\lambda_2)v_0^2 - 2cv_0.$$

The final result of the minimization process is given in the following table:

Magnitude	MINUIT value (MeV)	Experimental value (MeV)	Error
v_0	92.00	92	-3.52×10^{-7}
m_π	137.84	137	6.10×10^{-3}
m_a	980.00	980	-1.26×10^{-6}
m_σ	599.99	600	-1.66×10^{-5}
m_η	497.78	548	-9.16×10^{-2}
$m_{\eta'}$	968.20	958	1.06×10^{-2}
Γ_a	60.00	60	2.04×10^{-5}
Γ_σ	600.00	600	6.81×10^{-6}

All the requirements concerning the control parameters are satisfied at this global solution. The fit makes the cubic (in H) terms in (5) actually more relevant than the linear one. As a last point, the ψ angle is treated as a prediction. Experimentally [9], $\psi \simeq -18^\circ + \arctan \sqrt{2} \simeq -18^\circ + 54.7^\circ \approx 36.7^\circ$, while our result is $\psi_{\text{MINUIT}} \approx 35.46^\circ$, in excellent agreement.

3 Introducing the axial chemical potential

In order to introduce the axial chemical potential we have to recall that, just as the ordinary baryonic potential is introduced as the zero-th component of a vector field, the axial chemical potential μ_5 can be implemented as the time component of an axial-vector field. We follow the arguments for strange quark suppression [13] of parity breaking effects in fireballs created in heavy ion collisions. These arguments are based on Eq. (1) where due to the unavoidable left-right oscillations the mean value of strange quark axial charge is washed out as the strange quark mass is comparable with decay width of fireballs. Accordingly we will use axial chemical potential in the non-strange sector only.

At the level of the meson Lagrangian (5) it will appear through the action of the covariant derivative

$$\partial_\mu \rightarrow D_\mu = \partial_\mu - i\{\mathbf{I}_q \mu_5 \delta_{\mu 0}, \cdot\} = \partial_\mu - 2i\mathbf{I}_q \mu_5 \delta_{\mu 0}. \quad (11)$$

An extra piece which is proportional to μ_5 appears in the P -even Lagrangian

$$\Delta\mathcal{L} = \frac{i}{2}\mu_5 \text{Tr} [\mathbf{I}_q (\partial_0 H H^\dagger - H \partial_0 H^\dagger)] + \mu_5^2 \text{Tr} (\mathbf{I}_q H H^\dagger). \quad (12)$$

For non-vanishing μ_5 , we will assume isospin symmetry and thus, we impose to our solutions to have $v_u = v_d = v_q \neq v_s$. The corresponding gap equations are

$$M^2 - 2(\lambda_1 + \lambda_2)v_q^2 - \lambda_2 v_s^2 + cv_s + 2\mu_5^2 = 0, \quad (13)$$

$$v_s(M^2 - 2\lambda_2 v_q^2 - (2\lambda_1 + \lambda_2)v_s^2) + cv_q^2 = 0. \quad (14)$$

The correct solution is taken imposing the correct limit $v_q, v_s \rightarrow v_0$ when $\mu_5 \rightarrow 0$ (see Figure 1 for the μ_5 evolution of the solution).

It should be clear that the inclusion of μ_5 leads automatically to a source of parity violation in the low-energy effective theory. The consequences are far reaching; parity ceases to be a guidance for

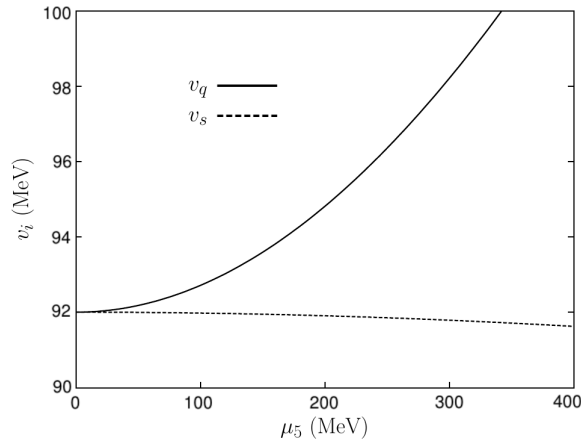


Figure 1: v_q and v_s dependence on μ_5 .

allowing/forbidding strong interaction processes, and states that have opposite parities, but otherwise equal quantum numbers, mix.

As an example of such a mixing let us consider the two isotriplets of opposite parity π and a_0 . After normalization of the states, let us consider the piece of the effective Lagrangian that is bilinear in the π and a_0 fields

$$\mathcal{L} = \frac{1}{2}(\partial a_0)^2 + \frac{1}{2}(\partial \pi)^2 - \frac{1}{2}m_1^2 a_0^2 - \frac{1}{2}m_2^2 \pi^2 - 4\mu_5 a_0 \dot{\pi}, \quad (15)$$

where

$$\begin{aligned} m_1^2 &= -2(M^2 - 2(3\lambda_1 + \lambda_2)v_q^2 - \lambda_2 v_s^2 - cv_s + 2(3d_1 + 2d_2)mv_q + 2d_2 m_s v_s + 2\mu_5^2), \\ m_2^2 &= \frac{2m}{v_q} [b + (d_1 + 2d_2)v_q^2 + d_2 v_s^2]. \end{aligned} \quad (16)$$

Notice that the resulting Lagrangian is not Lorentz invariant, which is obvious from (11). We will perform a diagonalization in momentum space, so the Lagrangian operator is written as

$$\mathcal{L} = -\frac{1}{2} \begin{pmatrix} a_0^*(k) & \pi^*(k) \end{pmatrix} \begin{pmatrix} -k^2 + m_1^2 & 4i\mu_5 k_0 \\ -4i\mu_5 k_0 & -k^2 + m_2^2 \end{pmatrix} \begin{pmatrix} a_0(k) \\ \pi(k) \end{pmatrix}. \quad (17)$$

Recall that fields in the momentum representation satisfy $A^*(k) = A(-k)$. Note also the fact that the mixing term has been rewritten as $-4\mu_5 a_0 \dot{\pi} = -2\mu_5 (a_0 \dot{\pi} - \dot{a}_0 \pi)$ in order the matrix to be hermitian. The eigenvalues are $\frac{1}{2}(k^2 - m_{\text{eff}}^2)$, where the (energy dependent) effective masses are

$$m_{\text{eff} \pm}^2(k_0) = \frac{1}{2} \left[m_1^2 + m_2^2 \pm \sqrt{(m_1^2 - m_2^2)^2 + (8\mu_5 k_0)^2} \right]. \quad (18)$$

The eigenstates are defined as

$$a_0 = \sum_j C_{aj} X_j, \quad \pi = \sum_j C_{\pi j} X_j, \quad C_{a1} = iC_{\pi 2} = C_+, \quad C_{a2} = -iC_{\pi 1} = -C_-, \quad (19)$$

with

$$C_{\pm} = \frac{1}{\sqrt{2}} \sqrt{1 \pm \frac{m_1^2 - m_2^2}{\sqrt{(m_1^2 - m_2^2)^2 + (8\mu_5 k_0)^2}}}. \quad (20)$$

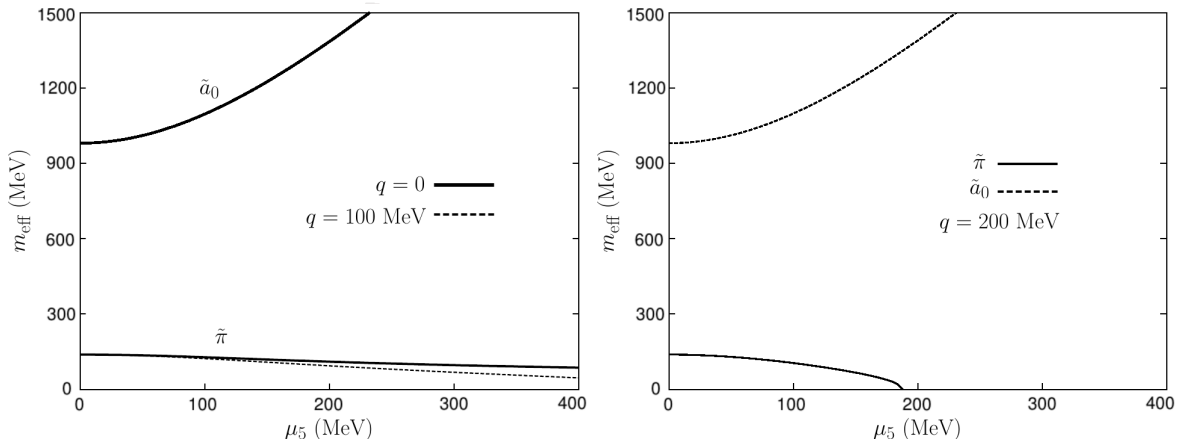


Figure 2: Effective mass dependence on μ_5 for $\tilde{\pi}$ and \tilde{a}_0 . Left panel: comparison of masses at rest and at low momentum $q = 100$ MeV. Right panel: masses at $q = 200$ MeV, where the $\tilde{\pi}$ mass goes tachyonic, as discussed in the text. For such momenta, the variations in \tilde{a}_0 are almost invisible and only slightly visible for large values of μ_5 for $\tilde{\pi}$.

We can also use the notation $X_1, X_2 \equiv \tilde{a}, \tilde{\pi}$, indicating that X_1 (resp. X_2) is the state that when $\mu_5 = 0$ goes over to a_0 (resp. π).

In Fig. 2, we present the results for the evolution of $\tilde{\pi}$ and \tilde{a}_0 effective masses with respect to the axial chemical potential μ_5 . As stressed, both states tend to the known physical ones in the limit $\mu_5 \rightarrow 0$. A remarkable feature of this model is the appearance of tachyonic states at high energies (or momenta). It is evident from Eq. (18) that for energies higher than a critical value $k_0, |\vec{k}| > m_1 m_2 / (4\mu_5) \equiv k_{\tilde{\pi}}^c$, the square root term dominates, thus leading to a negative squared mass for pions, as shown in the right panel of Fig. 2. Such a behaviour does not represent a serious physical obstacle since it can be checked that the energies are always positive and no vacuum instabilities appear. On the other hand, the \tilde{a}_0 mass shows an important enhancement, but in this model μ_5 has to be understood as a perturbatively small parameter, and very high values are beyond the domain of applicability of the effective Lagrangian. A better treatment of \tilde{a}_0 would require the inclusion of heavier degrees of freedom such as $\pi(1300)$ for instance.

4 Mixing $\eta - \sigma - \eta'$

A similar analysis applies to the isosinglet case. We shall consider three states here: η , η' and σ . As before, the starting point will be the piece of the effective Lagrangian (5) that after the inclusion of μ_5 is bilinear in the fields, i.e. the properly normalized kinetic part

$$\mathcal{L} = \frac{1}{2}[(\partial\sigma)^2 + (\partial\eta_q)^2 + (\partial\eta_s)^2] - \frac{1}{2}m_3^2\sigma^2 - \frac{1}{2}m_4^2\eta_q^2 - \frac{1}{2}m_5^2\eta_s^2 - 4\mu_5\sigma\eta_q - 2\sqrt{2}c v_q \eta_q \eta_s. \quad (21)$$

The constants appearing in the previous equation are given by

$$\begin{aligned} m_3^2 &= -2(M^2 - 6(\lambda_1 + \lambda_2)v_q^2 - \lambda_2 v_s^2 + c v_s + 6(d_1 + 2d_2)mv_q + 2d_2 m_s v_s + 2\mu_5^2), \\ m_4^2 &= \frac{2m}{v_q} [b + (d_1 + 2d_2)v_q^2 + d_2 v_s^2] + 2c v_s, \\ m_5^2 &= \frac{2m_s}{v_s} [b + 2d_2 v_q^2 + (d_1 + d_2)v_s^2] + \frac{c v_q^2}{v_s}. \end{aligned} \quad (22)$$

In matrix form

$$\mathcal{L} = -\frac{1}{2} \begin{pmatrix} \sigma^*(k) & \eta_q^*(k) & \eta_s^*(k) \end{pmatrix} \begin{pmatrix} -k^2 + m_3^2 & 4i\mu_5 k_0 & 0 \\ -4i\mu_5 k_0 & -k^2 + m_4^2 & 2\sqrt{2}cv_q \\ 0 & 2\sqrt{2}cv_q & -k^2 + m_5^2 \end{pmatrix} \begin{pmatrix} \sigma(k) \\ \eta_q(k) \\ \eta_s(k) \end{pmatrix}. \quad (23)$$

The equation for the eigenvalues (effective masses) is now a cubic one and the solution is determined numerically

$$-8c^2v_q^2(m_{\text{eff}}^2 - m_3^2) + (m_{\text{eff}}^2 - m_5^2) \left[\left(m_{\text{eff}}^2 - \frac{1}{2}(m_3^2 + m_4^2) \right)^2 - \frac{1}{4}(m_3^2 - m_4^2)^2 - (4\mu_5 k_0)^2 \right] = 0. \quad (24)$$

As before the eigenstates are defined via

$$\sigma = \sum_j C_{\sigma j} X_j, \quad \eta_q = \sum_j C_{\eta_{qj}} X_j, \quad \eta_s = \sum_j C_{\eta_{sj}} X_j, \quad (25)$$

where

$$C_{\sigma j} = \frac{4i\mu_5 k_0 (m_5^2 - m_j^2)}{N_j \prod_{k \neq j} (m_j^2 - m_k^2)}, \quad C_{\eta_{qj}} = \frac{(m_5^2 - m_j^2)(m_3^2 - m_j^2)}{N_j \prod_{k \neq j} (m_j^2 - m_k^2)}, \quad C_{\eta_{sj}} = \frac{-2\sqrt{2}cv_q (m_3^2 - m_j^2)}{N_j \prod_{k \neq j} (m_j^2 - m_k^2)}$$

$$\frac{1}{N_j} = \sqrt{1 + \frac{(4\mu_5 k_0)^2}{(m_j^2 - m_3^2)^2} + \frac{8c^2v_q^2}{(m_j^2 - m_5^2)^2}}. \quad (26)$$

N_j is the proper (eigen)field normalization factor.

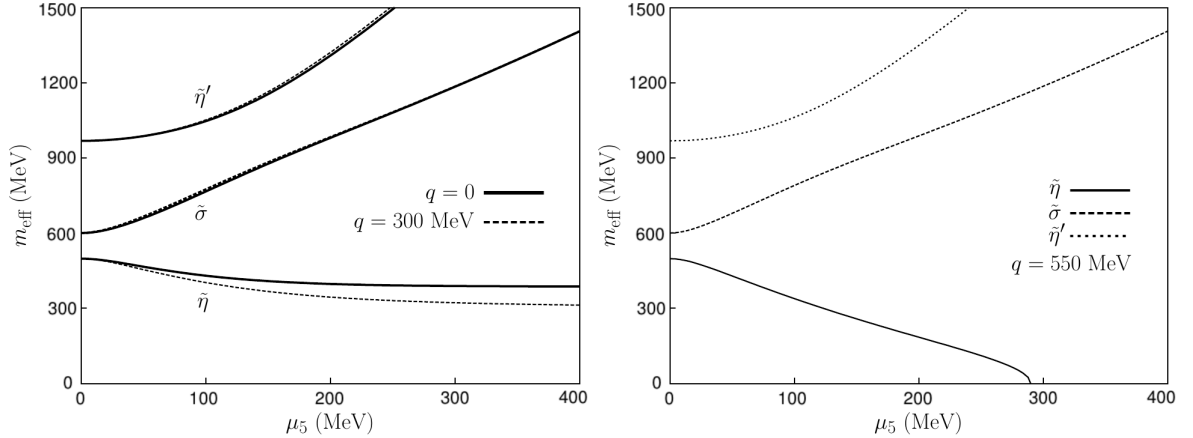


Figure 3: Effective mass dependence on μ_5 for $\tilde{\eta}$, $\tilde{\sigma}$ and $\tilde{\eta}'$. Left panel: comparison of masses at rest and at low momentum $q = 300$ MeV. Right panel: masses at $q = 550$ MeV, where the $\tilde{\eta}$ mass goes tachyonic, as discussed in the text. As in the previous example, for this range of momenta, the variations in the heavier degrees of freedom $\tilde{\sigma}$ and $\tilde{\eta}'$ are almost invisible and only slightly visible for large values of μ_5 for $\tilde{\eta}$.

The μ_5 -dependence of the effective masses is plotted in Fig. 3. As in the previous example, the lightest degree of freedom becomes tachyonic for big energies or momenta $k_0, |\vec{k}| > k_{\tilde{\eta}}^c$ with $k_{\tilde{\eta}}^c \equiv m_3/(4\mu_5 m_5) \sqrt{m_4^2 m_5^2 - 8c^2 v_q^2}$, as shown in the right panel of Fig. 3. The tachyon critical energy presents a similar behaviour as the one in the triplet case. In Fig. 4, both isotriplet $k_{\tilde{\pi}}^c$ and isosinglet critical energies $k_{\tilde{\eta}}^c$ are plotted together.

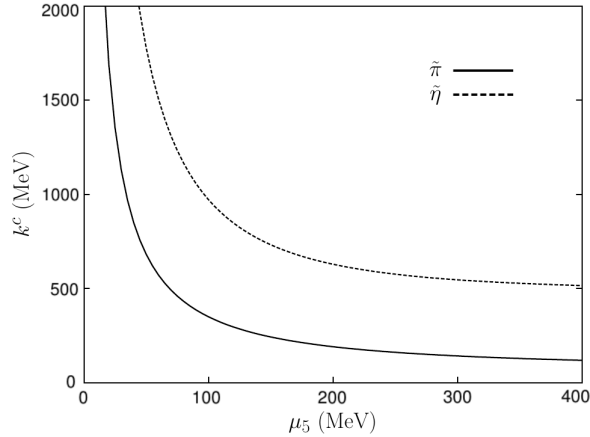


Figure 4: μ_5 -dependence of the tachyon critical energy for isotriplet $k_{\tilde{\pi}}^c$ and isosinglet case $k_{\tilde{\eta}}^c$.

5 New interactions and decay widths

After the inclusion of μ_5 the cubic couplings present in the effective Lagrangian (5) are

$$\begin{aligned}
\mathcal{L}_{\sigma aa} &= 2[(3d_1 + 2d_2)m - 2(3\lambda_1 + \lambda_2)v_q]\sigma\vec{a}^2, \\
\mathcal{L}_{\sigma\pi\pi} &= \frac{1}{v_q^2} [(\partial\vec{\pi})^2 v_q - (b + 3(d_1 + 2d_2)v_q^2 + d_2 v_s^2)m\vec{\pi}^2] \sigma, \\
\mathcal{L}_{\eta a\pi} &= \frac{2}{v_q^2} [\partial\eta_q \vec{a} \partial\vec{\pi} v_q - (b + (3d_1 + 2d_2)v_q^2 + d_2 v_s^2)m\eta_q \vec{a}\vec{\pi}], \\
\mathcal{L}_{\sigma a\pi} &= -\frac{4\mu_5}{v_q} \sigma \vec{a} \dot{\vec{\pi}}, \quad \mathcal{L}_{\eta aa} = -\frac{2\mu_5}{v_q} \eta_q \vec{a}^2, \quad \mathcal{L}_{\eta\pi\pi} = 0.
\end{aligned} \tag{27}$$

As seen in the previous expressions, decays that are normally forbidden on parity conservation grounds are now possible with a strength proportional to the parity breaking parameter μ_5 . However, the previous interaction terms are not physical because the properly diagonalized states are now X_i rather than the original fields π , a_0 , etc. Going to the physical basis requires using the diagonalization matrices defined in the previous section.

Our ultimate purpose is to check the relevance of dynamically generated parity breaking through topological charge fluctuations in heavy ion collisions. It is natural then to ask how the previously derived masses and vertices may influence the physics in the hadronic fireball.

It should be clear that the influence may be very important if μ_5 is such that the induced parity breaking effects are significant. After the initial collision of two heavy ions in a central or quasi-central process a fireball is formed. This fireball could be described in rather simplistic terms as a hot and dense pion gas. Pion-pion interaction is dominated by σ and ρ -particle exchanges and processes such as $\eta \rightarrow \pi\pi$ or $\eta' \rightarrow \pi\pi$ are forbidden. If parity is no longer a restriction, these two processes, or rather processes such as $X_i \rightarrow \tilde{\pi}\tilde{\pi}$ ($i = 3, 4, 5$) are for sure relevant and the new eigenstates produced due to parity breaking could thermalize inside the fireball.

Let us now try to be more quantitative. It should be clear from the mass evolution as a function of μ_5 (Figure 2) that $\tilde{\pi}$ is the lightest state and it dominates the partition function in the fireball. As a consequence, to get an estimate of the relevance of these new states let us compute their width in order to see whether its inverse is comparable to the fireball lifetime. To do so we need the following

S -matrix element corresponding to $X_i(q) \rightarrow \tilde{\pi}^+(p)\tilde{\pi}^-(p')$

$$\begin{aligned}
i\mathcal{M} = & 4i[(3d_1 + 2d_2)m - 2(3\lambda_1 + \lambda_2)v_q]C_{\sigma i}C_{a_2}^+C_{a_2}^- + \frac{4\mu_5}{v_q}C_{\sigma i}(E_{p'}C_{a_2}^+C_{\pi_2}^- + E_pC_{a_2}^-C_{\pi_2}^+) \\
& - \frac{i}{v_q^2}[(m_{X_i}^2 - m_{\tilde{\pi}^+}^2 - m_{\tilde{\pi}^-}^2)v_q + 2(b + 3(d_1 + 2d_2)v_q^2 + d_2v_s^2)m]C_{\sigma i}C_{\pi_2}^+C_{\pi_2}^- \\
& - \frac{4\mu_5E_q}{v_q}C_{\eta_q i}C_{a_2}^+C_{a_2}^- + \frac{i}{v_q}(m_{\tilde{\pi}^+}^2 - m_{\tilde{\pi}^-}^2)C_{\eta_q i}(C_{a_2}^-C_{\pi_2}^+ - C_{a_2}^+C_{\pi_2}^-) \\
& - \frac{i}{v_q^2}[2(b + (3d_1 + 2d_2)v_q^2 + d_2v_s^2)m - m_{X_i}^2v_q]C_{\eta_q i}(C_{a_2}^+C_{\pi_2}^- + C_{a_2}^-C_{\pi_2}^+) \tag{28}
\end{aligned}$$

We are dealing with a relativistic non-invariant theory and therefore the widths do not a priori transform as one would naively think. We shall compute them first at rest, then for different values of the 3-momentum of the decaying particle.

5.1 Widths at rest

The width of X_i is calculated from the amplitude shown before since we don't include further decaying processes. Recall that all masses are energy dependent. At the X_i rest frame, $\vec{q} = \vec{0}$ and $E_p = E_{p'} = m_{X_i}(\vec{q} = \vec{0})/2 \equiv m_0^{X_i}/2$. Here, a momentum-dependent effective mass is taken instead of an energy-dependent one since we assume the decaying particle to be on-shell so both $m(\vec{k})$ and $m(k_0)$ coincide. Thus, the rest width is given by

$$\Gamma_{X_i \rightarrow \tilde{\pi}\tilde{\pi}} = \frac{3}{2} \frac{1}{2m_0^{X_i}} |\mathcal{M}|^2 \frac{1}{4\pi} \frac{p_{\tilde{\pi}}}{m_0^{X_i} \frac{dp_{\tilde{\pi}}^2}{dE_p^2}}, \quad \frac{dp_{\tilde{\pi}}^2}{dE_p^2} = 1 + \frac{(4\mu_5)^2}{\sqrt{(m_1^2 - m_2^2)^2 + (8\mu_5 E_p)^2}} \tag{29}$$

where $p_{\tilde{\pi}}(E_p) = \sqrt{E_p^2 - m_{\tilde{\pi}}^2(E_p)}$ and the factor $3/2$ accounts for the decay both to neutral and charged $\tilde{\pi}$. The results of the widths are shown in Figure 5.

The new state $\tilde{\eta}$ exhibits a smooth behaviour with an average value ~ 60 MeV, corresponding to a mean free path ~ 3 fm, which is smaller than the typical fireball size $L_{\text{fireball}} \sim 5 \div 10$ fm. Hence, the thermalization of this channel via regeneration of $\tilde{\pi}$ within the gas seems to be possible.

Another striking point concerning $\tilde{\sigma}$ takes place down to $\mu_5 \sim 100$ MeV, when the decay width decreases dramatically leading to scenarios where this state becomes stable. The visible bumps in these two latter channels seem to reflect the tachyonic nature of the decaying $\tilde{\pi}$.

Finally, we present in the inset of Fig. 5 the detail of the $\tilde{\eta}'$ width, that grows up to the GeV scale, showing clear violations of unitarity. As in the case of \tilde{a}_0 , more hadronic degrees of freedom are needed to obtain a reliable result, such as $f_0(980)$, etc.

5.2 Decay widths of moving particles

Next, let us compute the width when the decaying particle is not at rest. As explained before in a non-relativistic theory this cannot be obtained from the one at rest by simply taking into account the time dilatation effect. Then

$$\Gamma_{X \rightarrow \tilde{\pi}\tilde{\pi}} = \frac{3}{2} \frac{1}{2E_q} \frac{1}{8\pi q} \int \frac{|\mathcal{M}|^2 p dp}{E_p \frac{dp_{\tilde{\pi}}^2}{dE_p^2}} \Theta(1 - |\cos \theta|) \Theta(E_{p'}) \tag{30}$$

where the Heaviside step functions are introduced to make sure that both $\cos \theta$ and $E_{p'}$ take physical values in the numerical calculation. Of course, the limit $q \rightarrow 0$ coincides with the calculation at rest performed before.

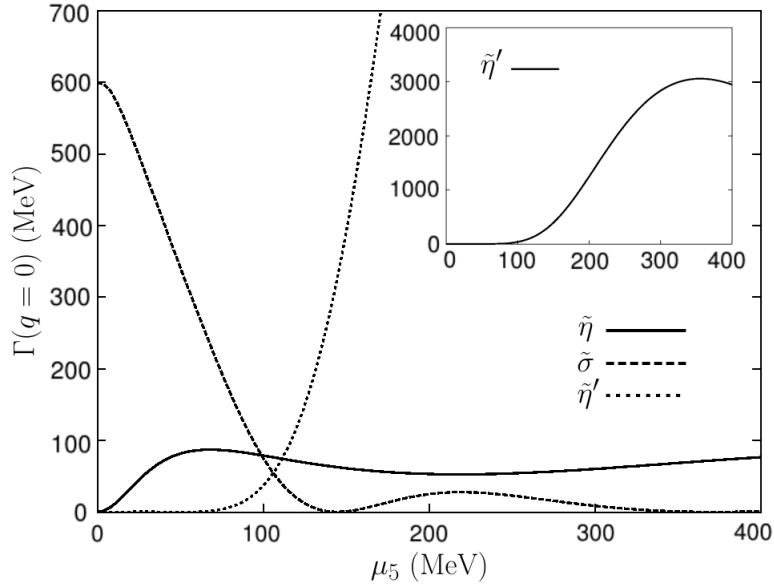


Figure 5: $\tilde{\eta}$, $\tilde{\sigma}$ and $\tilde{\eta}'$ widths at rest depending on μ_5 . Down to $\mu_5 = 50$ MeV, $\tilde{\eta}$ acquires a width of order 60 MeV, with a characteristic mean free path smaller than the typical fireball size of $5 \div 10$ fm and hence implying that thermalization may occur in this channel. Nevertheless, $\tilde{\sigma}$ shows a pronounced fall and beyond $\mu_5 = 100$ MeV, it becomes a stable channel. Inset: Detail of $\tilde{\eta}'$ width reaching the GeV scale, a clear violation of unitarity since we don't include heavier degrees of freedom in our model.

In the $\tilde{\eta}$ channel (see the left section of Fig. 6), one may observe small variations at low 3-momenta with respect to the width at rest, namely, two initial bumps at $\mu_5 \sim 80$ MeV and 550 MeV (the latter being beyond the plot range) slowly separate as one increases q . However, the two-dimensional representation $\Gamma_{\tilde{\eta}}(\mu_5, q)$ exhibits a saddle point around $\mu_5^* \sim 240$ MeV and $q^* \sim 500$ MeV, and in consequence, for large 3-momenta, a third intermediate bump appears opening the possibility of creating two different tachyons at the same time. The latter maximum grows fast as one increases q and becomes the global one when the 3-momentum goes beyond $q \gtrsim 700$ MeV.

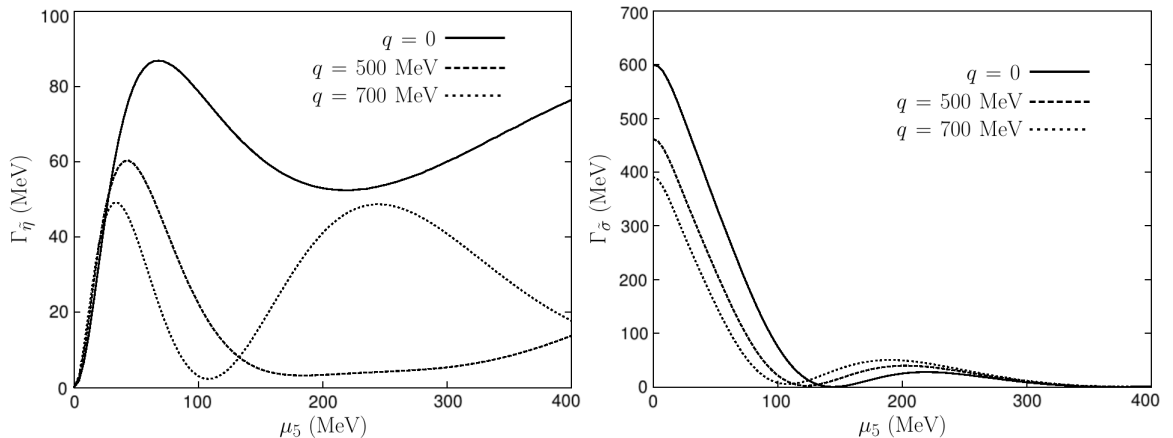


Figure 6: $\tilde{\eta}$ (left) and $\tilde{\sigma}$ (right) widths depending on μ_5 for different values of the incoming 3-momentum: $q = 0, 500, 700$ MeV. The first plot shows a non-trivial dependence on q (see text) while the second one shows a fall that is mainly due to the Lorentz factor.

On the other hand, in the $\tilde{\sigma}$ and $\tilde{\eta}'$ channels no huge differences arise when boosting the decaying

particle. In the right panel of Fig. 6, we show the $\tilde{\sigma}$ width for different values of q and the most salient behaviour is, as in the previous case, the separation of the two minima as one increases q .

6 Axial-vector meson condensation

The introduction of axial chemical potential into the quark-meson model interferes with the flavor-singlet axial-vector channel as this potential is just a time component of axial-vector field, $\Delta\mathcal{L}_{\mu_5} = \mu_5 \bar{q} \gamma_0 \gamma_5 \mathbf{I}_q q$. Therefore if one includes the coupling of the singlet axial-vector quark current with the corresponding meson field h_μ one expects mixing and renormalization of the bare axial chemical potential due to condensation of the time components of the axial-vector fields $h^\mu \simeq \langle h^0 \rangle \delta^{0\mu}$. This phenomenon is in full analogy to the condensation of the time component of the ω meson field when a baryon chemical potential enters the Lagrangian [14] which is quite important to understand the repulsive nuclear forces in this channel.

Let us elucidate this phenomenon in more details. The relevant Lagrangian for axial-vector mesons reads

$$\Delta\mathcal{L} = -\frac{1}{4} h_{\mu\nu} h^{\mu\nu} + \frac{1}{2} m_h^2 h_\mu h^\mu + \bar{q} \gamma_\mu \gamma_5 (g_h h^\mu + \delta^{\mu 0} \mu_5) \mathbf{I}_q q, \quad (31)$$

where h stands for the axial-vector meson $h_1(1170)$ [9] singlet in flavor and g_h denotes its coupling to the quark current. We assume the condensation of $h^\mu \simeq \langle h^0 \rangle \delta^{0\mu}$

$$\frac{\delta\Delta\mathcal{L}}{\delta h_0} = m_h^2 \langle h_0 \rangle + g_h \langle \bar{q} \gamma_0 \gamma_5 \mathbf{I}_q q \rangle = 0, \quad (32)$$

so that the effective chemical potential $\bar{\mu}_5 \equiv \mu_5 + g_h \langle h_0 \rangle$ arises and determines the effective non-strange axial-charge density $\rho_5 = \langle \bar{q} \gamma_0 \gamma_5 \mathbf{I}_q q \rangle$

$$\rho_5(\bar{\mu}_5) = \frac{\mu_5 - \bar{\mu}_5}{G_h} = \frac{\delta\Delta\mathcal{L}}{\delta\bar{\mu}_5}, \quad \Delta V = -\frac{1}{2} m_h^2 \langle h_0 \rangle^2 = -\frac{1}{2} \frac{(\bar{\mu}_5 - \mu_5)^2}{G_h}, \quad (33)$$

where $G_h = g_h^2/m_h^2$. Therefrom we can see that the axial charge density is directly related to the axial-vector condensate. After including ΔV (Eq. (33)) in Eq. (12) the stationary point equation can be derived

$$\frac{\delta\mathcal{L}}{\delta\bar{\mu}_5} = \frac{\delta}{\delta\bar{\mu}_5} \left[2\bar{\mu}_5^2 v_q^2 + \frac{1}{2} \frac{(\bar{\mu}_5 - \mu_5)^2}{G_h} \right] = 0 \quad (34)$$

that allows to relate the bare and effective axial chemical potentials

$$\bar{\mu}_5 [1 + 4G_h v_q^2] = \mu_5. \quad (35)$$

We stress that in the mass-gap equations for v_q, v_s the effective axial chemical potential $\bar{\mu}_5$ must be used. The relation (35) is smooth against the decoupling of axial-vector mesons $g_h \rightarrow 0$. It determines unambiguously the axial charge density, $\rho_5(\bar{\mu}_5) = 4\bar{\mu}_5 v_q^2(\bar{\mu}_5)$, which exhibits, in general, lower values when affected by axial meson forces, $|\bar{\mu}_5| < |\mu_5|$.

7 Conclusions and outlook

Perhaps the main conclusion of the study of meson physics in an environment endowed with a net axial charge is that is full of surprises. The axial chemical potential provides a source of parity violation. This makes states of different intrinsic parities mix and allows for ‘exotic’ processes in hadronic physics. The presence of the axial charge also leads unavoidably to a breaking of Lorentz invariance. The effective in-medium masses are energy dependent and meson physics is frame-dependent, with the natural consequence that widths or decay rates do depend non-trivially on the momentum of the decaying particle.

We have assumed that the parity breaking parameter -the axial chemical potential- is an $SU(2)$ singlet. This is natural if the mechanism to generate μ_5 is via topological charge fluctuations as advocated by some [4, 6]. Note, however, that it is not an $SU(3)$ singlet, as the topological charge fluctuations are not transmitted to the strange sector (and even less to the eventual charm sector).

It is natural to ask whether such a mixing of states of different parities occurs in the vector/axial-vector sector. There are many models dealing with vector particles phenomenologically. If we assume that the vector mesons appear as part of a covariant derivative (as postulated e.g. in hidden symmetry models [15]), no mixing term can be generated by operators of dimension 4 if μ_5 is an isosinglet. However, such a mixing is not forbidden on (global) symmetry grounds if μ_5 is present, appearing as the time component of an axial-vector field (see e.g. [12]). This means that this coupling is very much model dependent and, unfortunately, not much phenomenological information is present. It is however an interesting point we plan to analyze in the future.

However parity breaking via a topological charge or axial chemical potential influences vector mesons (and eventually photons too) in a different way discussed in detail in [13]. Their polarizations are severely distorted and the breaking of Lorentz invariance, together with parity, reflects itself in different polarizations acquiring different effective masses, which could hopefully be experimentally measured. This issue has not been discussed here.

As argued in the introduction, many authors support the idea that topological charge fluctuations may lead to visible effects via the Chiral Magnetic Effect. If this is so, not only peripheral collisions (where the Chiral Magnetic Effect is present) will show traces of parity breaking. We have argued elsewhere [13, 16] that parity breaking induced from topological charge fluctuation will lead to possibly measurable effects in central collisions, in the dilepton spectrum from ρ and ω decays.

What we have seen in the work presented here is that the physics of spin zero resonances is also strongly affected by the presence of an axial chemical potential. We have given convincing arguments that, if $\mu_5 \neq 0$ the pion gas in the fireball forming after a central heavy ion collision may actually not be made of the usual pions, but instead of some states of non-defined parity and energy-dependent effective mass. In addition all the lightest spin zero states have the same properties and perhaps more importantly, they are all in thermal equilibrium with the ‘pion’ gas, as indicated by the characteristic large widths, completely different from the ones in vacuum. These particles have Dalitz decays that are therefore completely distorted with respect to the $\mu_5 = 0$ case usually considered. This phenomenon may help in explaining the anomalous dilepton yield enhancement observed [17] for low dilepton invariant masses in heavy ion collisions.

Acknowledgements

We acknowledge the financial support from projects FPA2010-20807, 2009SGR502, CPAN (Consolider CSD2007-00042). A. A. Andrianov is also supported by Grant RFBR 10-02-00881-a. X. Planells acknowledges the support from Grant FPU AP2009-1855.

References

- [1] D. Weingarten, Phys. Rev. Lett. 51, 1830 (1983); C. Vafa and E. Witten, Phys. Rev. Lett. 53 (1984) 535; S. Nussinov, Phys. Rev. Lett. 52, 966 (1984); D. Espriu, M. Gross and J.F. Wheeler, Phys. Lett. B 146, 67 (1984); for a review see, S. Nussinov and M. Lambert, Phys. Rept. 362 (2002) 193.

- [2] A. A. Andrianov, D. Espriu, Phys. Lett. B 663 (2008) 450; A. A. Andrianov, V. A. Andrianov, D. Espriu, Phys. Lett. B 678 (2009) 416.
- [3] M. P. Lombardo, PoS CPOD 2006 (2006) [hep-lat/0612017]; M. A. Stephanov, PoS LAT2006 (2006) 024 [hep-lat/0701002]; D. T. Son and M. A. Stephanov, Phys. Rev. Lett. 86 (2001) 592; Phys. Atom. Nucl. 64 (2001) 834; K. Splittorff, D. T. Son, and M. A. Stephanov, Phys. Rev. D 64 (2001) 016003; J. B. Kogut and D. Toublan, Phys. Rev. D 64 (2001) 034007.
- [4] D. Kharzeev, R. D. Pisarski, M. H. G. Tytgat, Phys. Rev. Lett. 81 (1998) 512; D. Kharzeev, Phys. Lett. B 633 (2006) 260; Ann. Phys. (NY) 325 (2010) 205; ; D. E. Kharzeev, L. D. McLerran, H. J. Warringa, Nucl. Phys. A 803 (2008) 227; K. Fukushima, D. E. Kharzeev, H. J. Warringa, Phys. Rev. D 78, 074033 (2008); Nucl. Phys. A 836 (2010) 311.
- [5] A. M. Polyakov, Nucl. Phys. B 120 (1977) 429.
- [6] D. Kharzeev, A. Zhitnitsky, Nucl. Phys. A 797 (2007) 67.
- [7] P. V. Buividovich, M. N. Chernodub, E. V. Luschevskaya, M. I. Polikarpov, Phys. Rev. D 80 (2009) 054503; P. V. Buividovich, M. N. Chernodub, D. E. Kharzeev, T. Kalaydzhyan, E. V. Luschevskaya, M. I. Polikarpov, Phys. Rev. Lett. 105 (2010) 132001; M. Abramczyk, T. Blum, G. Petropoulos and R. Zhou, PoS LAT 2009, 181 (2009) [arXiv:0911.1348 [hep-lat]]; P.V. Buividovich, T. Kalaydzhyan, M.I. Polikarpov [arXiv:1111.6733v2 [hep-lat]].
- [8] B. I. Abelev et al. [STAR Collaboration], Phys. Rev. Lett. 103, 251601 (2009); S. A. Voloshin, J. Phys. Conf. Ser. 230, 012021 (2010).
- [9] J. Beringer et al. [Particle Data Group], Review of Particle Physics, Phys. Rev. D86 (2012) 010001.
- [10] J. Boguta, Phys. Lett. B 120 (1983) 34; O. Kaymakcalan and J. Schechter, Phys. Rev. D 31 (1985) 1109; R. D. Pisarski, arXiv:hep-ph/9503330.
- [11] A. H. Fariborz, R. Jora and J. Schechter, Phys. Rev. D 72, 034001 (2005); Phys. Rev. D 77, 034006 (2008).
- [12] J.T. Lenaghan, D.H. Rischke, J. Schaffner-Bielich, Phys.Rev.D62, 085008 (2000); D. Parganlija, F. Giacosa and D.H. Rischke, Phys. Rev. D 82, 054024 (2010).
- [13] A. A. Andrianov, V. A. Andrianov, D. Espriu and X. Planells, Phys. Lett. B 710 (2012) 230.
- [14] B. D. Serot and J. D. Walecka, Int. J. Mod. Phys. E 16 (1997) 15.
- [15] M. Bando, T. Kugo, and K. Yamawaki, Phys. Rep. 164,(1988) 217; M. Harada and K. Yamawaki, Phys. Rep. 381 (2003) 1.
- [16] A. A. Andrianov, V. A. Andrianov, D. Espriu, X. Planells, PoS QFTHEP2010, 053 (2010); AIP Conf. Proc. 1343 (2011) 450.
- [17] K. O. Lapidus, V. M. Emel'yanov, Phys. Part. Nucl. 40 (2009) 29; I. Tserruya, Electromagnetic Probes, arXiv: 0903.0415 [nucl-ex]; R. Arnaldi et al. [NA60 Collaboration], Eur. Phys. J. C 61 (2009) 711; A. Adare et al. [PHENIX Collaboration], Phys. Rev. C 81, 034911 (2010).